# Characterization of Class-E Resonant Converter Operating in MHz-Range

I. Krois and A. Barić
University of Zagreb, Faculty of Electrical Engineering and Computing, Zagreb, Croatia
adrijan.baric@fer.hr

***Abstract* - A class-E resonant converter operating at 2 MHz is designed and characterized. The values of the inductive and capacitive components used in the designed converter are calculated using a set of mathematical equations. Time-domain measurements are performed to analyze the steady-state operation of the designed converter and to verify an impact of the converter parameters on the zero-voltage-switching behavior. An impact of switching frequency on output voltage and impact of duty cycle on zero-voltage-switching effect is analyzed. Finally, conducted electromagnetic emissions of the converter are measured at the nominal operating point.**

***Index Terms* - *DC-DC converter, electromagnetic emissions, switching power supply, zero-voltage switching***

## I. INTRODUCTION

Reduction of physical dimensions of switching power converters is the major reason for the on-going attempts to push the operating frequency of switching power converters to higher values [1]. The conventional topologies of switching power converters suffer from hard-switching effects that cause a rather large switching loss. Furthermore, due to the rich spectrum of their switching voltage and current waveforms, fast switching converters conduct noise currents back to the power line at the harmonics of the switching frequency and cause conducted and radiated electromagnetic emissions [2].

The zero-voltage switching (ZVS) and zero-voltage-derivative switching (ZVDS) effects that occur in the class-E resonant converters significantly reduce switching losses ad generated EM emissions caused by the switching behavior of the converter [3].

The methodology used to calculate inductive and capacitive components used to shape the time-domain voltage and current waveforms of a transistor and a diode for a specified operating condition of a resonant converter is described in detail in [4], while a unified design theory for various topologies of the class-E resonant converter is proposed in [5]. An impact of inductors having different inductances, case sizes, saturation currents and quality factors on the operation of a resonant converter is simulated in SPICE and presented in [6].

In this paper, a non-isolated class-E resonant DC-DC converter designed to operate at 2 MHz is presented. The values of the inductive and capacitive components used in the converter are calculated using the analytical method described in [4]. The time-domain measurements and estimation of conducted EM emissions are performed to characterize the operation of the designed converter.

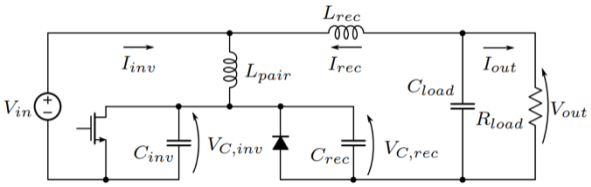


Fig. 1. Schematic of a non-isolated class-E resonant converter [7].

Section II presents the designed class-E resonant converter. The time-domain measurement results and conducted EM emissions are presented in Section III. Conclusion is given in Section IV.

## II. DESIGNED CLASS-E RESONANT DC-DC CONVERTER

A schematic representation of a non-isolated class-E resonant converter analyzed in this paper is shown in Fig. 1 [7]. The converter is designed to operate at 12-V input voltage, 5-V output voltage, 1-A output current ($R_{load}$ = 5 Ω) and switching frequency of 2 MHz. A 100-V N-channel MOSFET from Vishay [8] is used in the inverter side of the converter, while a PMEG6030ELPX Schottky diode with a current rating of 3 A is used as a free-wheeling Schottky diode in the rectifier side. A 5-Ω SMD load resistor is used to define the nominal output current of 1 A.

The design of the converter, i.e. the calculation of the inductive and capacitive components ($L_{pair}$, $L_{rec}$, $C_{inv}$ and $C_{rec}$) is performed using the state-of-the art methodology presented in [4]. Denormalized values of the converter that are obtained are the following: $L_{pair} = L_{rec}$ = 1.68 µH, $C_{inv}$ = 3.82 nF, $C_{rec}$ = 0.86 nF.

A converter is designed on a dual-sided printed circuit board (PCB) which enables its insertion into the 62-pin connector to the 100 mm x 100 mm motherboard that can be used for far-field estimation in a (G)TEM cell. The values of the inductive and capacitive components that are soldered to the PCB, i.e. used in the assembled resonant converter, are the following: $L_{pair} = L_{rec}$ = 1.5 µH, $C_{inv}$ =

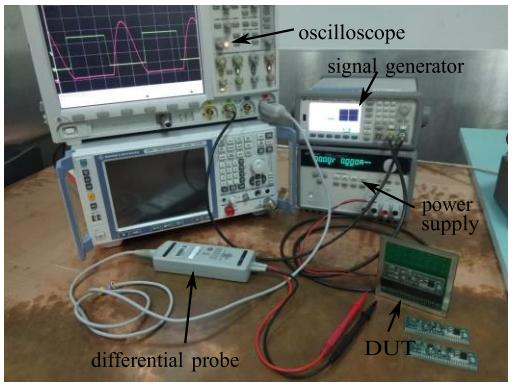


Fig. 2. Photo of the measurement setup for time-domain measurements.

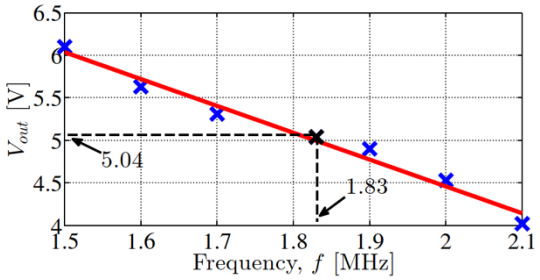


Fig. 3. Measured output voltage of the designed converter at different switching frequencies.

3.90 nF, $C_{rec}$ = 0.82 nF.

## III. Measurement Results

### A. Time-domain

The measurement setup used for time-domain characterization of the designed resonant converter is shown in Fig. 2. A signal generator is used to generate a 2-MHz pulse signal for the operation of the transistor switch. The driver circuit is supplied by the 12-V DC voltage that is separated from the input voltage of the designed converter to enable the control of the input voltage.

The voltage across $C_{inv}$, i.e. the drain-source voltage of the transistor, and the voltage across $C_{rec}$, i.e. the Schottky diode, are measured using a differential voltage probe having a bandwidth of 100 MHz. Time-domain waveforms of the currents through $L_{pair}$ and $L_{rec}$ are measured using the high-sensitivity clamp-on current probe attached to the pieces of wire placed in series to the 1.5-µH inductors. A misalignment between the time delays of voltage and current probe is corrected using the deskew fixture [9]. The time-domain voltage and current waveforms are recorded using a 4-channel oscilloscope.

An impact of the switching frequency of the designed converter on the measured output voltage is shown in Fig. 3. The output voltage of the converter at 2-MHz switching frequency is measured to be 4.53 V, while 5.04 V at the output of the converter is achieved at switching frequency of 1.83 MHz. This discrepancy between measured and calculated data can be attributed to the large impact of the component parameters, due to the tolerance and parasitics,

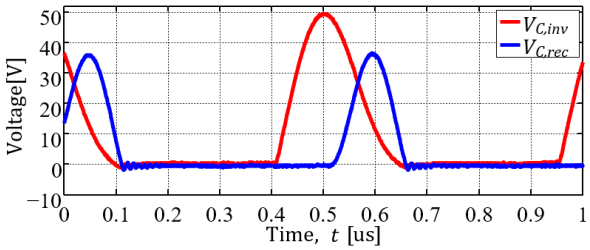


Fig. 4. Time-domain waveforms of the voltages across transistor $V_{C,inv}$ and diode $V_{C,rec}$ ($D$ = 54%).

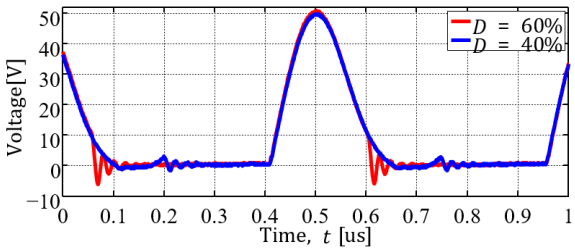


Fig. 5. Voltage across the transistor $V_{C,inv}$: impact of the duty cycle $D$ on ZVS effect.

on the operation of the resonant converter.

The power efficiency η of the converter is estimated at 1.83 MHz and the output voltage of 5.04 V as follows:

$$\eta = \frac{V_{OUT}^2/R_L}{V_{IN} \cdot I_{IN}} = \frac{5.04^2/5.09}{11.89 \cdot 0.988} = 0.425 = 42.5\%.$$

The input and output voltage of the converter are measured using the digital multimeter, while the input current is measured by the DC voltage source applied to the input of the converter. The load resistance $R_{load}$ of 5.09 Ω is measured using the precise four-point measurement method. This relatively low value of converter efficiency is due to losses in the ferrite cores of the used coils. These are coils that are commercially available and have a more favorable ratio of operating frequency, rated current and core volume. Increasing the efficiency of the converter should go in the direction of using RF air coils while increasing the frequency of the converter.

The time-domain waveforms of the voltages across the transistor switch ($V_{C,inv}$ in Fig. 1) and across the diode ($V_{C,rec}$ in Fig. 1) are shown in Fig. 4. The converter is set to reduce the 12-V input voltage to 5-V output voltage, but the peak values of 50 V across the transistor and almost 40 V across the diode can be observed, which puts a stringent limitation on capacitor selection in terms of breakdown voltage.

A slow increase from zero and slow decrease to zero value of the voltages across transistor and a diode at their turn-on and turn-off events indicate that ZVS operation of the designed converter is achieved. The waveforms shown in Fig. 4 correspond to the duty cycle of 54% at which the smoothest waveforms and lowest oscillations are obtained. An impact of the duty cycle on the time-domain waveform of the voltage across the transistor can be observed in Fig. 5. It can be seen that both increase or decrease of the duty ratio from the nominal value causes a significant increase

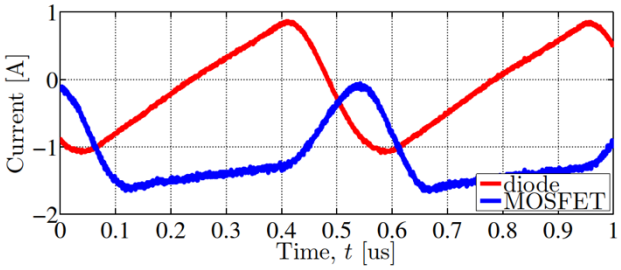


Fig. 6. Time-domain waveforms of the currents flowing through transistor and diode.

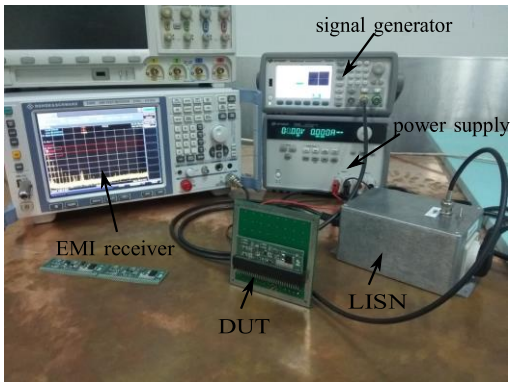


Fig. 7. Photo of the measurement setup used for estimation of conducted EM emissions.

of the oscillations observed in time-domain waveforms.

Finally, the time-domain waveforms of the currents flowing through the transistor and the diode are measured using the clamp-on current probe and shown in Fig. 6.

### *B. Conducted EM emissions*

The measurement setup used for estimation of conducted EM emissions generated by the designed converter is shown in Fig. 7. The conducted emissions are measured between 150 kHz and 30 MHz using the EMI receiver and an average detector, 9-kHz RBW filter, logarithmic frequency sweep with 10 sweep counts and 8001 points per one frequency sweep.

The conducted EM emissions are measured for the input voltage of 12 V, switching frequency of 1.83 MHz and duty cycle of 54%, which produced the output voltage of 5.04 V. The red curve in Fig. 8 shows the noise generated by the measurement setup when the converter is switched off. The blue curve shows the measured conducted EMI voltage. The spectrum consists of the fundamental frequency at 1.83 MHz and odd harmonics. The limit lines for conducted emissions according to the CISPR standard are shown in black.

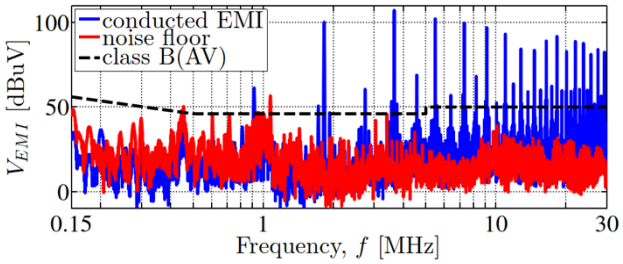


Fig. 8. Conducted EMI voltage of the designed resonant converter.

## IV. CONCLUSION

A class-E resonant DC-DC converter that reduces the 12-V input voltage to the 5-V output voltage is designed and characterized. The designed converter operates at 1.83 MHz, while the duty cycle of 54% is selected to obtain the smoothest transitions between the on-and off-state. It is observed that the shift of the duty cycle from the nominal value causes a significant increase of the oscillations at the voltage waveforms. The conducted EM emissions of the converter are measured at the nominal operating point.

## ACKNOWLEDGEMENT

This work is supported by the Croatian Science Foundation (HRZZ) within the project Fast switching converters based on GaN devices and resonant architectures (IP-2019-04-8959).

## REFERENCE

[1] R. Erickson and D. Maksimovic, *Fundamentals of Power Electronics*, 2nd ed. Kluwer Academic Publishers, 2001.

[2] H. Ott, *Electromagnetic Compatibility Engineering*, 1st ed. Wiley, 2009.

[3] M. Kazimierczuk and D. Czarkowski, *Resonant Power Converters*, 2nd ed. Wiley-IEEE Press, 2011.

[4] Bertoni, Nicola and Frattini, Giovanni and Massolini, Roberto G. and Pareschi, Fabio and Rovatti, Riccardo and Setti, Gianluca, "An Analytical Approach for the Design of Class-E Resonant DC-DC Converters," *IEEE Transactions on Power Electronics*, vol. 31, no. 11, pp. 7701–7713, 2016.

[5] F. Pareschi, N. Bertoni, M. Mangia, R. Rovatti, and G. Setti, "A Unified Design Theory for Class-E Resonant DC-DC Converter Topologies," *IEEE Access*, vol. 7, pp. 83 825–83 838, 2019.

[6] J. Bačmaga, R. Blečić, F. Pareschi, R. Rovatti, G. Setti, and A. Barić, "Frequency-Domain Characterization of Power Inductors for Class-E Resonant Converters," in *IEEE 23rd Workshop on Signal and Power Integrity (SPI)*, 2019, pp. 1–4.

[7] N. Bertoni, G. Frattini, P. Albertini, F. Pareschi, R. Rovatti, and G. Setti, "A First Implementation of a Semi-Analytically Designed Class-E Resonant DC-DC Converter," in *IEEE International Symposium on Circuits and Systems (ISCAS)*, 2015, pp. 221–224.

[8] *N-Channel 100 V (D-S) MOSFET – Si2392ADS*, Vishay, 2014, available at https://www.vishay.com/.

[9] *R&S RT-ZF20 Power Deskew Fixture*, Rohde&Schwarz, 2019, available at https://www.rohde-schwarz.com/.